



## Stabilization treatment of arsenic-alkali residue (AAR): Effect of the coexisting soluble carbonate on arsenic stabilization



Xin Wang<sup>a,b</sup>, Jiaqi Ding<sup>a</sup>, Linling Wang<sup>a,\*</sup>, Shuyuan Zhang<sup>a</sup>, Huijie Hou<sup>a</sup>, Jingdong Zhang<sup>b</sup>, Jing Chen<sup>a,\*</sup>, Miao Ma<sup>c</sup>, Daniel C.W. Tsang<sup>d</sup>, Xiaohui Wu<sup>a</sup>

<sup>a</sup> Environmental Science Research Institute, School of Environmental Science and Engineering, Huazhong University of Science and Technology, Wuhan 430074, China

<sup>b</sup> School of Chemistry and Chemical Engineering, Huazhong University of Science and Technology, Wuhan 430074, China

<sup>c</sup> Zhongnan Engineering Corporation Limited, Changsha 410000, China

<sup>d</sup> Department of Civil and Environmental Engineering, The Hong Kong Polytechnic University, Hung Hom, Kowloon, Hong Kong, China

### ARTICLE INFO

Handling Editor: Da Chen

#### Keywords:

Arsenic-alkali residue

Arsenic stabilization

Ferrous sulfate

Lime

Arsenate minerals

Coexisting soluble carbonate

### ABSTRACT

Arsenic-alkali residue (AAR) from antimony smelting is highly hazardous due to its ready leachability of As, seeking for proper disposal such as stabilization treatment. However, As stabilization in AAR would be challenging due to the high content of coexisting soluble carbonate. This study conducted the stabilization treatments of AAR by ferrous sulfate and lime, respectively, and revealed the significant influence of coexisting carbonate. It was found that ferrous sulfate was more efficient than lime, which required only one-tenth of dosages of lime to reduce the As leaching concentration from 915 mg/L to a level below 2.5 mg/L to meet the Chinese regulatory limit. The combining qualitative and quantitative analyses based on XRD, SEM-EDS, and thermodynamic modeling suggested that the formation of insoluble arsenate minerals, ferrous arsenate or calcium arsenate, was the predominant mechanism for As stabilization in the two treatment systems, and their efficiency difference was primarily attributed to the coexisting carbonate, which had a slight effect on ferrous arsenate but severely obstructed calcium arsenate formation. Moreover, the examination of As leaching concentrations in 1-year-cured samples indicated that the long-term stability of ferrous sulfate treatment was far superior to that of lime treatment. This study provides ferrous salts as a promising and green scheme for stabilization treatment of AAR as well as other similar As-bearing solid wastes with coexisting soluble carbonate.

### 1. Introduction

Arsenic-alkali residue (AAR) from antimony (Sb) smelting is a highly hazardous arsenic-bearing solid waste with a high content of available arsenic (As) (1–10%) (Guo et al., 2014; Zeng et al., 2011), which could generate severe threats to ecological environment and human health (Wang et al., 2013; Wen et al., 2018). The AAR problem is faced by all Sb producing countries such as China, Burma, Russia, Bolivia, Tajikistan, and South Africa; among these countries, China is the most serious country owing to its highest Sb production that accounts for almost 80% of the world share (Multani et al., 2016). Due to the lack of cost-effective, efficient, and reliable treatment technologies for AAR disposal, the majority of AAR has not yet been adequately handled.

Commonly, stabilization technologies are adopted to reduce the environmental risk of As-bearing solid wastes (e.g., tailings, fly ash, sludge, and sediment) (Beiyan et al., 2017; Liang et al., 2017; Randall,

2012; Renew et al., 2016; Wang et al., 2019a; Wang et al., 2019b). For example, Liang et al. studied the stabilization treatment of As-bearing sludge from wastewater treatment using MnO<sub>2</sub> modified zero-valent iron (Liang et al., 2017), and Wang et al. investigated As stabilization in sediment by adding Si-rich minerals and reactive MgO (Wang et al., 2019a). Previous studies have only focused on As stabilization effectiveness and As species transformation triggered by added agents, but little attention was paid to the effect of coexisting components on As stabilization. Due to the high content of coexisting soda (Na<sub>2</sub>CO<sub>3</sub>, 20–30%) (Anderson, 2012; Deng et al., 2014), As stabilization in AAR may differ from that in the mentioned As-bearing solid wastes. Nowadays, there is still a lack of knowledge for the stabilization of As-bearing solid wastes with extremely high contents of soluble carbonate.

Lime and ferrous salts have been widely used for As stabilization due to their high efficiency and low cost (Kumpiene et al., 2008; Miretzky and Cirelli, 2010). Lime treatment could transform available As to insoluble Ca–As precipitates/minerals, such as Ca<sub>3</sub>(AsO<sub>4</sub>)<sub>2</sub>·2H<sub>2</sub>O,

\* Corresponding authors.

E-mail addresses: [wanglinling@hust.edu.cn](mailto:wanglinling@hust.edu.cn) (L. Wang), [chenjing@hust.edu.cn](mailto:chenjing@hust.edu.cn) (J. Chen).

<https://doi.org/10.1016/j.envint.2019.105406>

Received 28 July 2019; Received in revised form 28 November 2019; Accepted 9 December 2019

Available online 19 December 2019

0160-4120/© 2019 The Authors. Published by Elsevier Ltd. This is an open access article under the CC BY-NC-ND license

(<http://creativecommons.org/licenses/by-nc-nd/4.0/>).

$\text{Ca}_5(\text{AsO}_4)_3\text{OH}$ , and  $\text{Ca}_4(\text{OH})_2(\text{AsO}_4)_2 \cdot 4\text{H}_2\text{O}$ , reducing the As leaching toxicity of solid wastes (Bothe and Brown, 1999a; Li et al., 2018; Moon et al., 2004; Wang et al., 2019c). Recently, a solution experiment demonstrated that carbonate anion could hinder the formation of calcium arsenate minerals by capturing  $\text{Ca}^{2+}$  to generate calcium carbonate minerals (Lei et al., 2018). Based on this result, the applicability of lime to AAR stabilization would be questionable due to the coexisting soluble carbonate in AAR.

For ferrous salts stabilization treatment, ferrous iron (Fe(II)) generally acts as a precursor of Fe(III) (hydr)oxides for As adsorption and coprecipitation (Cao et al., 2016; Li et al., 2012; Tong et al., 2014; Yang et al., 2007). Carbonate anion reportedly has a negative effect on As immobilization via competing with As, especially under high carbonate concentration conditions (Arai et al., 2004; Kanematsu et al., 2011; Stachowicz et al., 2007). Thus, As stabilization in AAR via adsorption and coprecipitation with Fe(III) (hydr)oxides from Fe(II) oxidation would be challenging owing to the presence of extremely high content of soluble carbonate. Perhaps the direct formation of ferrous arsenate precipitates/minerals could be another stabilization pathway in alkaline AAR, based on the suggestion of Johnston and Singer that ferrous arsenate is a significant sink for As(V) in some alkaline waters (Johnston and Singer, 2007). But the effect of coexisting carbonate on ferrous arsenate precipitation remains unknown. Accordingly, the utilization of ferrous salts and lime for AAR stabilization requires a systematic investigation focusing on the specific stabilization processes and coexisting carbonate's effect, so as to develop a green and efficient scheme for stabilization treatment of AAR.

In this study, the evaluation and comparison of the performance of ferrous sulfate and lime for As stabilization in AAR were done based on the change of As leaching concentrations. More importantly, the effect of coexisting carbonate on insoluble arsenate minerals formation is investigated via mineralogical characterization and thermodynamic modeling, aiming to clarify the specific mechanisms for As stabilization in the context of AAR with a high content of soluble carbonate.

## 2. Materials and methods

### 2.1. Materials and chemicals

The AAR sample was collected from an abandoned Sb ore smelter in Hunan, China. The sample was homogenized, air-dried and sieved to a size fraction < 2 mm for later use. Ferrous sulfate heptahydrate ( $\text{FeSO}_4 \cdot 7\text{H}_2\text{O}$ ), calcium oxide (CaO), sulfuric acid ( $\text{H}_2\text{SO}_4$ ), nitric acid ( $\text{HNO}_3$ ), and other reagents were obtained from Sinopharm Chemical Reagent (China). All of the chemicals were of analytical grade. Deionized water (18.2 M $\Omega$  cm) obtained from a Millipore Milli-Q system was used throughout the experiments.

### 2.2. Stabilization treatments

Ferrous sulfate and lime (calcium oxide) were used for AAR stabilization treatments. During stabilization processes, the raw AAR sample of 100 g (based on dry solids) were firstly mixed with a desired amount of stabilizing agents ( $\text{FeSO}_4 \cdot 7\text{H}_2\text{O}$  or CaO) and 40 mL of water in a plastic bottle using a spatula for 10 min of repeated stirring, and then naturally cured in a ventilated place at room temperature. The low liquid-to-solid ratio (0.4 mL/g) was adopted to avoid an undesired liquid-solid separation. Water contents of the treated samples were less than 20% after natural curing. All samples were prepared in duplicate.

After 7 days of natural curing, As leaching concentrations of the treated AAR samples were assessed by the standard leaching procedure of China (HJ/T299–2007). In order to simulate the leaching situation under acid rain exposure, a  $\text{H}_2\text{SO}_4/\text{HNO}_3$  (mass ratio = 2/1) solution with pH  $3.20 \pm 0.05$  was used as the extraction solution in this method. Briefly, each 10 g of solid samples were mixed with a certain amount of extraction solution depended on the water contents of solid

samples to obtain a final liquid-to-dry solid ratio of 10 (mL/g), then the mixture was oscillated in a capped polypropylene bottle on a rotary tumbler at  $30 \pm 2$  rpm for  $18 \pm 2$  h ( $23 \pm 2$  °C). After extraction, the leachates were filtered through a 0.22  $\mu\text{m}$  nylon membrane for the measurements of final pH and aqueous As concentrations. Some samples were cured in a ventilated place at room temperature for 1 year before the leaching procedure to investigate the long-term stability of treated AAR. The long-term stability in this study was appraised by the alteration of As leaching concentrations after 1 year of natural curing (Wang et al., 2017).

### 2.3. Analyses and characterization

Arsenic concentrations in filtered solution samples after acidification were analyzed by inductively coupled plasma optical emission spectrometry (ICP–OES) with an Optima 8300 system (PerkinElmer, USA). As(III) and As(V) in the solutions were measured by an atomic fluorescence spectrophotometer (AFS 9600, Beijing Haiguang, China) combined with a high performance liquid chromatography (HPLC) system for separation of As(III) and As(V), where a Hamilton PRP–X100 anion-exchange column (10  $\mu\text{m}$ , 4.1  $\times$  250 mm) was used (Zhong et al., 2019).

The total As content of the raw AAR sample was determined via a digestion method of aqua regia (Wang et al., 2016). Soluble and adsorbed As contents were measured by water and  $\text{Na}_2\text{HPO}_4$  extraction experiments as shown in Supplementary Material S1. The pH values of solid samples were based on a water-to-solid ratio of 2.5 (mL/g). The soluble carbonate content of the raw AAR sample was analyzed via a water extraction experiment at a water-to-dry solid ratio of 10 (mL/g), and the water extraction procedure was similar to the leaching procedure in Section 2.2. After extraction, the supernatant liquid was filtered by a 0.22  $\mu\text{m}$  nylon membrane for carbonate concentration measurement by a TOC analyzer (Multi C/N 2100, Analytik Jena, Germany) under a mode of total inorganic carbon (TIC) measurement. Then, the soluble carbonate content in AAR could be calculated by multiplying the carbonate concentration in the extract by the water-to-dry solid ratio.

Elemental composition was characterized by X-ray fluorescence (XRF) spectrometry (EAGLE III, EDAX, USA). Mineralogical characterization was investigated by powder X-ray diffraction (XRD) analysis (XRD–7000, Shimadzu, Japan) with a copper target (Cu–K $\alpha$ ). The equipment was operated by step-scanning from 10° to 70° with a scan speed of 2°/min at 40 kV and 30 mA. The morphology of newly formed minerals was determined using Pt coated samples and a ZEISS Sigma 300 scanning electron microscope (SEM) equipped with a Bruker energy dispersive spectroscopy (EDS) system. Surface properties were characterized by X-ray photoelectron spectroscopy (XPS, AXIS–ULTRA DLD–600W, Shimadzu, Japan) with a monochromatic Mg–K $\alpha$  source. The charge effect was corrected using the C1s line at 284.8 eV and the curve-fitting program XPSPEAK 4.1 was applied to fitting the spectra.

### 2.4. Thermodynamic modeling

In order to reveal the role of precipitation of arsenate and carbonate minerals for As stabilization in AAR, a thermodynamic model was established using MINEQL+ (Version 4.6) (Schecher and McAvoy, 2007), mainly based on precipitation reactions of Fe(II)–arsenate, Fe(II)–carbonate, Ca–arsenate, and Ca–carbonate. Concentrations of aqueous As and yields of arsenate and carbonate precipitates as a function of the dosages of ferrous iron and lime were calculated. Aqueous concentrations, precipitate yields, and stabilizing agent dosages were all based on the liquid-to-dry solid ratio of 10, which was consistent with the leaching procedure. Initial concentrations of  $\text{AsO}_4^{3-}$  and  $\text{CO}_3^{2-}$  were set at 0.012 mol/L (915 mg/L of As) and 0.203 mol/L, respectively. The detailed equilibrium reactions and associated equilibrium constants are presented in Table S1.

**Table 1**  
Main characteristics of the raw AAR.

Parameters	Values
As leaching concentration (mg/L)	915
Total As (mg/kg)	15,750
Soluble As (mg/kg)	9025
Soluble carbonate (mol/kg)	2.03
pH	10.9
Other elements (wt%) <sup>a</sup>	
Si	18.0
Sb	10.7
Na	10.7
Al	6.8
Fe	5.5
Ca	3.7
Zn	1.5
Sn	1.3
Ti	0.4
Mn	0.1

<sup>a</sup> The contents of other elements were from XRF analysis.

### 3. Results and discussion

#### 3.1. Characteristics of AAR

The main characteristics of the raw AAR sample are summarized in Table 1. The total As content in the sample was 15750 mg/kg, with Si (18.0 wt%), Sb (10.7 wt%), Na (10.7 wt%), Al (6.8 wt%), Fe (5.5 wt%), and Ca (3.7 wt%). The XPS As3d analysis (Fig. S1) indicated that As(V) was the unique valence of As in the AAR, in agreement with the literature (Deng et al., 2014; Li et al., 2015). The As leaching concentration of AAR was 915 mg/L (Table 1), which was much higher than the limit values of Chinese standard (2.5 mg/L) as well as international standards from the European Union, the United Kingdom, and America (Table S2). In the leachate, only As(V) was detected by HPLC-AFS, which was consistent with the XPS result (Fig. S1). The leachable As was about 58.1% of the total As content, which was comparable to the fraction of soluble As (57.3%) (Table 1). The content of soluble carbonate in the AAR was as high as 2.03 mol/kg AAR as shown in Table 1, which was about 17 times of soluble arsenate. The high content of soluble carbonate in AAR stems from unreacted soda ( $\text{Na}_2\text{CO}_3$ ) during Sb pyrometallurgical processes (Fig. S2). Because of these  $\text{Na}_2\text{CO}_3$ , AAR was high-alkaline and the pH value of AAR was 10.9 (Table 1). Additionally, mopungite, senarmonite, cancrinite, and quartz were found to be the main minerals in the AAR, and no As-bearing minerals were observed (Fig. S3).

#### 3.2. Arsenic stabilization by ferrous sulfate and lime

Arsenic leaching concentrations in the treated AAR were significantly reduced (Fig. 1a,b), demonstrating the stabilization effects of ferrous sulfate and lime. The As leaching concentration in the ferrous iron system reduced more rapidly than that in the lime system as the dosages of stabilizing agents were increased. In the ferrous iron system, As leaching concentration sharply dropped from initial 915 mg/L to below the regulatory limit of 2.5 mg/L at the dosage of 0.5 mol/kg (Fig. 1a inset). By comparison, lime treatment at the same dosage (0.5 mol/kg) left behind a high As leaching concentration of 881 mg/L which was close to the original value (915 mg/L) (Fig. 1b), indicating that the addition of lime at lower amounts had a slight effect on As stabilization. Only when the higher amount of lime (5.0 mol/kg) was employed, As leaching concentration was reduced to below 2.5 mg/L (Fig. 1b inset). The minimum requirement of Fe/As and Ca/As molar ratios for meeting the regulatory limit were calculated to be 4 and 40, respectively, based on the leachable As content of 0.122 mol/kg. In our previous study about the stabilization of realgar tailings by ferrous

sulfate, the minimum requirement of Fe/As molar ratio was about 40 which was much higher than that of here (Wang et al., 2019). According to comparison, we concluded that ferrous sulfate matched better with AAR relative to realgar tailings, and it was more efficient than lime for AAR stabilization.

As shown in Fig. 1c,d, the final pH values of the two treatments were entirely different, which were depended on the properties of stabilizing agents. Ferrous iron treatment reduced pH values to a neutral range, while lime treatment made AAR more alkaline. For example, 0.5 mol/kg of ferrous iron resulted in a pH reduction to 7.5 from 10.9 (Fig. 1c); oppositely, lime with a dosage of 5.0 mol/kg elevated the pH value to 12.3 (Fig. 1d). The ferrous iron-treated AAR with neutral pH was environmentally acceptable, whereas the lime-treated AAR would harm to the surrounding environment due to its ultrahigh alkalinity. Therefore, ferrous iron treatment was the greener scheme for AAR stabilization.

The leaching concentrations of other heavy metals were also examined after the stabilization treatments by ferrous iron and lime (Table 2). According to the standard for hazardous waste landfills (GB 18598–2001, China EPA), all required heavy metals (As, Ba, Be, Cd, Cr, Cu, Hg, Ni, Pb, and Zn) met the regulatory limits after treatments. Although Sb was not included in the standard, Sb leaching concentrations were also monitored in this study, considering the high content of Sb in AAR and its potential environmental risks. The leaching concentration of Sb (10.2 mg/L) in the raw AAR was far below that of As (915 mg/L) (Table 2), suggesting that As is the main pollutant needing to be stabilized in AAR. After treatment, the Sb leaching concentrations reduced to 6.65 and 5.41 mg/L in the ferrous iron system and lime system, respectively (Table 2). These results indicated that over half of leachable Sb was not effectively stabilized as the stabilization of leachable As achieved more than 99.8%. As a result of the ultimate disposal of treated AAR into hazardous waste landfills, the leachable Sb would be finally concentrated in landfill leachates, where Sb should be considered as an essential object for removal. Even so, ferrous iron and lime were still competent in AAR treatment to meet the standard.

The costs of the two treatments were simply evaluated here. The market prices of each ton ferrous sulfate and lime were about 28 and 50 US dollars, respectively. According to Fig. 1a,b, the cost-effective dosages of ferrous sulfate and lime were 0.5 and 5.0 mol/kg, so the corresponding costs for treating each ton AAR were about 4 and 14 US dollars, respectively. Ferrous sulfate was the more economical agent for the stabilization treatment of AAR.

#### 3.3. Formation of arsenate and carbonate minerals

Based on the XRD and SEM-EDS characterization (Figs. 2 and 3), two newly formed ferrous minerals, symplectite ( $\text{Fe}_3(\text{AsO}_4)_2 \cdot 8\text{H}_2\text{O}$ , PDF #00-008-0172) and siderite ( $\text{FeCO}_3$ , PDF #01-083-1764), were detected in the ferrous iron-treated AAR at the dosage of 0.5 mol/kg. The XPS analysis in the Fe2p region supported the formation of ferrous minerals, where Fe(II) accounting for 29% of the total Fe was measured (Fig. 4). Symplectite was spherical aggregates with a coarsely fibrous, radial structure (Fig. 3a), whereas siderite had a monolithic shape (Fig. 3b). The measured As/Fe atomic ratio of symplectite by EDS (Fig. 3e) was 0.64 that was close to the theoretical ratio of 0.67. Symplectite is a ferrous arsenate mineral with low solubility ( $\text{p}K_{\text{sp}} = 33.25$ ) (Johnston and Singer, 2007), so it could be responsible for As stabilization in the ferrous iron-treated AAR. Reports of symplectite formation during stabilization treatment of As-bearing solid wastes were scarce, although symplectite has been identified in As-bearing wastewater treatment (Daenzer et al., 2015; Daenzer et al., 2014). This study could be an essential supplement. Symplectite is formed only under conditions of high initial concentrations of arsenate and ferrous iron (Catalano et al., 2011; Daenzer et al., 2014). Thus, the AAR's nature with a high content of soluble arsenate is the critical condition for symplectite formation.

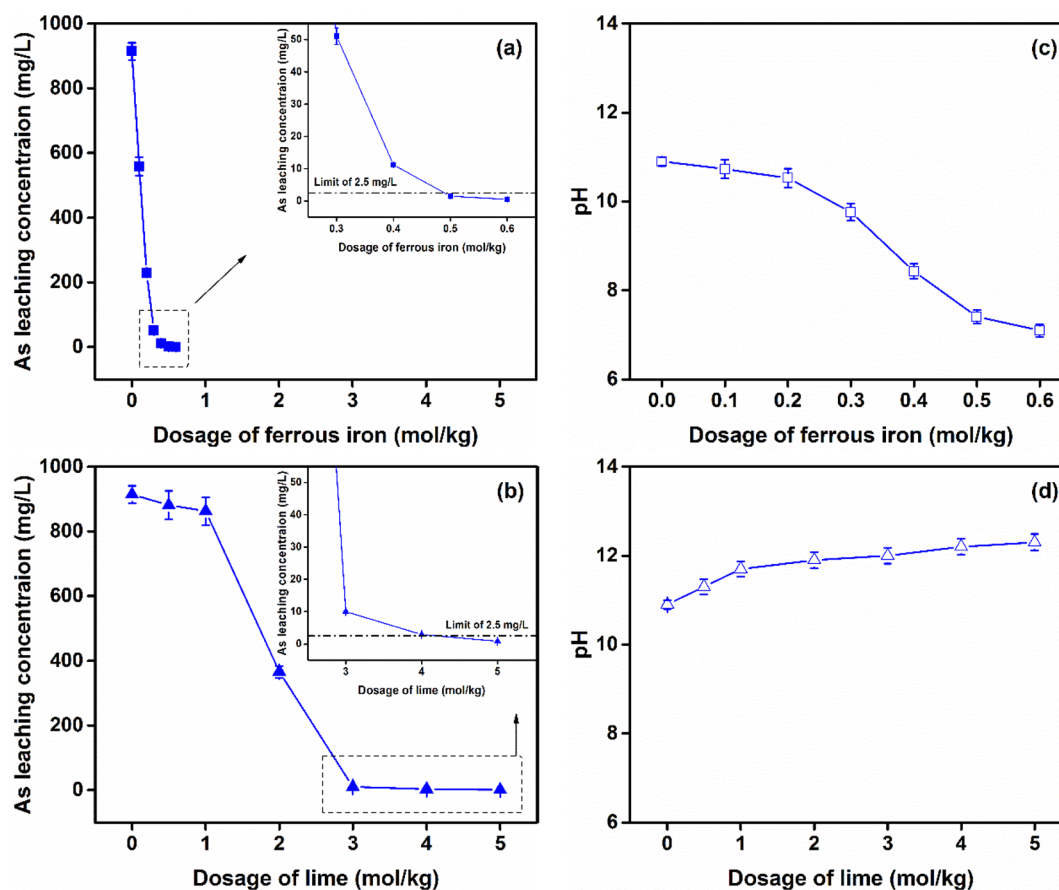


Fig. 1. Variations of As leaching concentration and pH as a function of dosages of (a, b) ferrous iron (as  $\text{FeSO}_4$ ) and (c, d) lime for AAR stabilization treatment after 7 days of curing.

Table 2

Leaching concentrations of selected heavy metals.

Heavy metals	Leaching concentrations (mg/L) <sup>a</sup>			Limit values (mg/L) <sup>b</sup>
	AAR	AAR-Fe-0.5	AAR-Ca-5.0	
As	915	1.53	0.80	2.5
Ba	0.03	0.04	0.02	150
Be	ND	ND	ND	0.2
Cd	0.37	0.05	0.10	0.5
Cr	ND	ND	ND	12
Cu	0.17	0.12	0.28	75
Hg	ND	ND	ND	0.25
Ni	ND	ND	ND	15
Pb	ND	ND	ND	5
Zn	0.10	0.29	0.59	75
Sb	10.2	6.65	5.41	–

<sup>a</sup> ND: not detected. Concentrations of Be, Cr, Ni, and Pb were measured by inductively coupled plasma optical emission spectrometry (ICP-OES), and detection limits are 0.005, 0.01, 0.01, and 0.05 mg/L for Be, Cr, Ni, and Pb, respectively. Atomic fluorescence spectrometry (AFS) was used for Hg analysis with a detection limit of 0.0001 mg/L.

<sup>b</sup> The limit values were required by the standard for hazardous waste landfills (GB 18598-2001, China EPA) in which Sb was not included.

Moreover, the alkaline pH induced by the soluble carbonate in AAR was in favor of the formation of symplectite, which was more stable at pH around 7–10 (Fig. S4a). The formed symplectite at the initial alkaline pH could well explain the remarkable reduction of As leaching concentration at the low ferrous iron dosage of 0.1 mol/kg (Fig. 1a), where the pH value was as high as 10.7 (Fig. 1c). Although high pH strongly restrains As adsorption and coprecipitation with Fe(III) (hydr)oxides

(Huo et al., 2017; Pan et al., 2018), it fails to hinder symplectite precipitation.

After lime treatment (5 mol/kg), calcium arsenate hydrate ( $\text{Ca}_3(\text{AsO}_4)_2 \cdot 2\text{H}_2\text{O}$ , PDF #00–017–0739) with a hexagonal shape was newly formed (Figs. 2 and 3). The  $\text{p}K_{\text{sp}}$  value of calcium arsenate hydrate is as high as 21.0 (Bothe and Brown, 1999b; Zhu et al., 2006), which should be responsible for the reduction of As leaching concentrations. Formation of Ca–As minerals is a widely accepted stabilization mechanism of As by lime treatment (Chen et al., 2015; Kundu and Gupta, 2008; Moon et al., 2004). Besides the arsenate mineral, two carbonate minerals, calcite and gaylussite, were generated as well. Calcite ( $\text{CaCO}_3$ ) is a common insoluble carbonate mineral with a  $\text{p}K_{\text{sp}}$  value of 8.47 (Haynes, 2014), while gaylussite ( $\text{Na}_2\text{Ca}(\text{CO}_3)_2 \cdot 5\text{H}_2\text{O}$ ) is slightly soluble in water and transforms readily to calcite. According to Fig. 1b, the stabilization of As by lime under low dosage conditions (< 2 mol/kg) was unsatisfactory. This result may be ascribed to the formation of carbonate minerals, which would consume a considerable amount of calcium from lime, suppressing the formation of Ca–As mineral (Lei et al., 2018).

In order to reveal the role of the formation of arsenate and carbonate minerals for As stabilization in AAR, the thermodynamic model was established (Fig. 5). In this thermodynamic model, the precipitation of Fe(II)–arsenate, Fe(II)–carbonate, Ca–arsenate and Ca–carbonate were primarily taken into account, while As adsorption and Fe(II) oxidation were assumed to be negligible based on the measurement of adsorbed As and XPS Fe2p analysis. The adsorbed As in the ferrous iron-treated AAR accounted for 12.0%, which was only 5.2% higher than that in the raw AAR (Table S3), indicating that As adsorption was just the minor stabilization mechanism in the ferrous iron treated AAR. According to the XPS Fe2p analysis (Fig. 4), less than 20% of added Fe

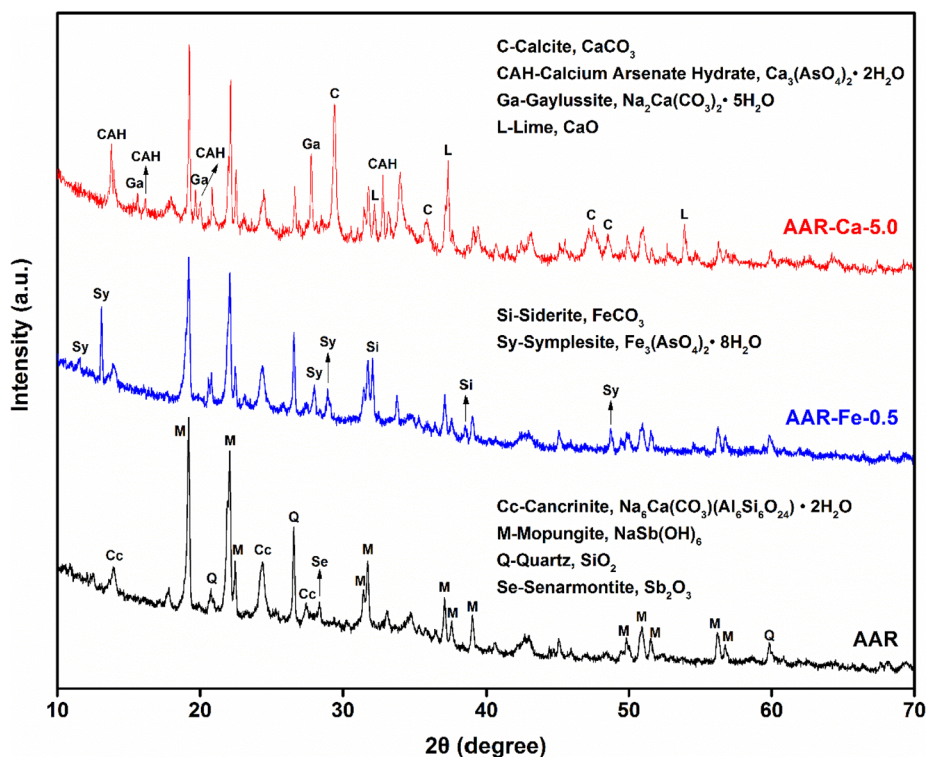


Fig. 2. Comparison of XRD patterns of the raw AAR and treated AAR after 7 days of curing. The dosages of ferrous iron (as  $\text{FeSO}_4$ ) and lime were 0.5 and 5.0 mol/kg AAR, respectively.

(II) was oxidized after 7 days, and the majority of added iron remained in the original state of Fe(II), which might be the reason for the less significant As adsorption. In general, the kinetic constant for Fe(II) oxidation is several orders of magnitude lower than that for Fe(II) precipitation (Crittenden et al., 2012). Daenzer et al. also found that only a small part of Fe(II) (< 10%) was oxidized during neutralization of acidic Fe(II)–As(V) solutions, and the bulk of Fe(II) was transferred into precipitates (Daenzer et al., 2014). Meanwhile, the adsorption capacity of calcium materials for As was actually weak (Jones and

Loeppert, 2013; Sø et al., 2008), resulting in that As adsorption cannot dominate As stabilization in the lime-treated AAR as well. Therefore, the formation of insoluble As precipitates was more likely to be the principal stabilization mechanism of As in the treated AAR.

The model calculation results well matched with the experimental findings in both ferrous iron and lime systems with  $R^2$  values of 0.94 and 0.98, respectively (Fig. 5a,b). Thus, this model was reasonably accurate to predict As stabilization in the treated AAR by both ferrous iron and lime, indicating that As stabilization was mostly attributed to

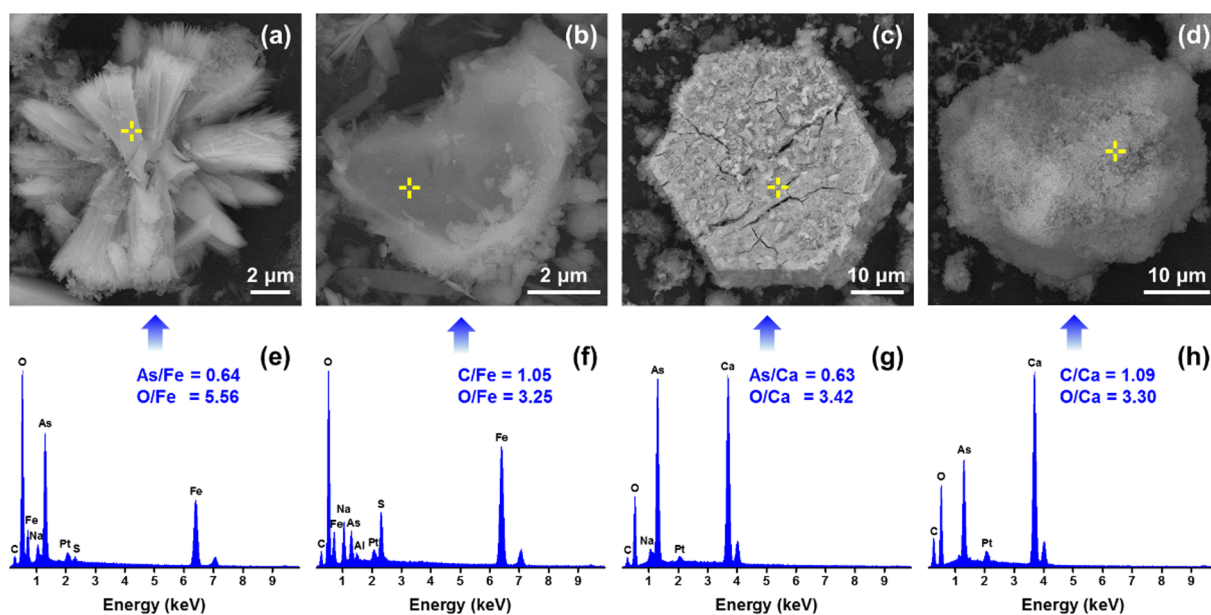


Fig. 3. SEM images of newly formed minerals (a–d) and their corresponding X-ray energy dispersive spectra (e–h) in the two treatment systems: (a, e)  $\text{Fe}_3(\text{AsO}_4)_2 \cdot 8\text{H}_2\text{O}$ , (b, f)  $\text{FeCO}_3$ , (c, g)  $\text{Ca}_3(\text{AsO}_4)_2 \cdot 2\text{H}_2\text{O}$ , and (d, h)  $\text{CaCO}_3$ . Based on the EDS data, the atomic ratios of specific elements were provided. The detailed element percent in EDS data (e–h) is shown in Table S4.

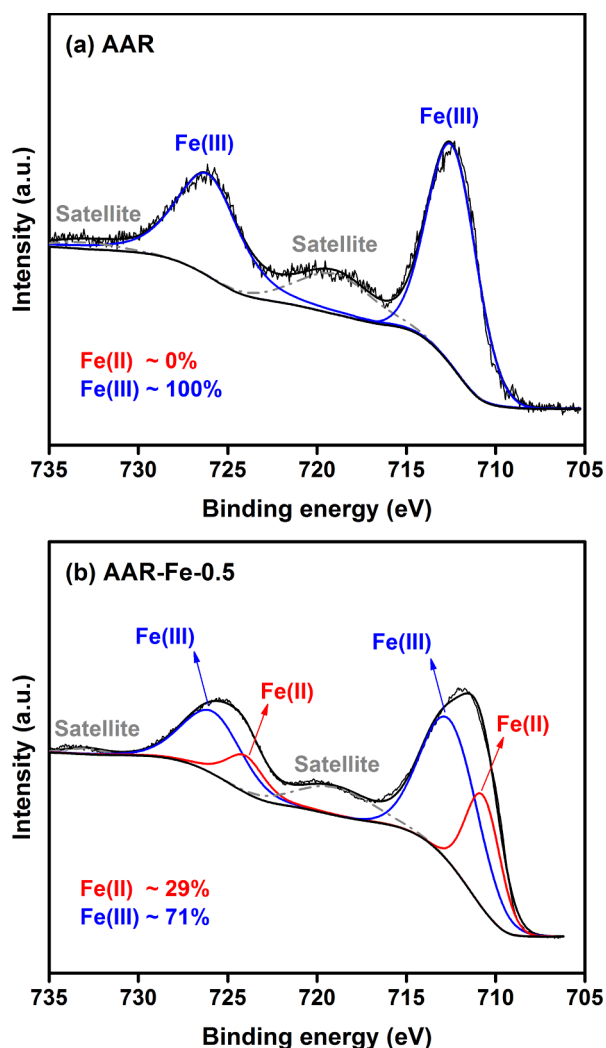


Fig. 4. XPS surveys of Fe2p for the (a) raw AAR and (b) treated AAR by ferrous iron (as  $\text{FeSO}_4$ ) of 0.5 mol/kg AAR after 7 days of curing.

insoluble arsenate minerals.

### 3.4. Effect of the coexisting soluble carbonate

The distinct difference of As stabilization efficiency between ferrous iron and lime treatments (Fig. 1a,b) could be well explained by the formation sequences of arsenate and carbonate minerals (Fig. 5c,d). In the lime system, the formation of calcite ( $\text{CaCO}_3$ ) was prior to calcium arsenate hydrate ( $\text{Ca}_3(\text{AsO}_4)_2 \cdot 2\text{H}_2\text{O}$ ) (Fig. 5d). Calcium arsenate hydrate could not be formed when the dosages of lime were below 1.9 mol/kg (Fig. 5d). This was consistent with the XRD results that only carbonate minerals were detected at the low dosage of lime (1.0 mol/kg) (Fig. S5). Therefore, the coexisting carbonate in AAR blocked the As stabilization process by consuming the added lime to form  $\text{CaCO}_3$  instead of  $\text{Ca}_3(\text{AsO}_4)_2 \cdot 2\text{H}_2\text{O}$  until carbonate precipitates were saturated by excess lime addition. In other words,  $\text{CO}_3^{2-}$  was a serious rival to  $\text{AsO}_4^{3-}$ . The content of soluble carbonate (2.03 mol/kg) was much higher than soluble arsenate content (0.12 mol/kg) in AAR, resulting in a significant increase of the amount of lime required for As stabilization (Fig. 1b).

Conversely, the formation of symplectite ( $\text{Fe}_3(\text{AsO}_4)_2 \cdot 8\text{H}_2\text{O}$ ) had priority over that of siderite ( $\text{FeCO}_3$ ) in the ferrous iron system (Fig. 5c). Siderite started to form only after the saturation of symplectite with the dosages of ferrous iron higher than 0.2 mol/kg, indicating that  $\text{CO}_3^{2-}$  was almost unable to compete with  $\text{AsO}_4^{3-}$  for  $\text{Fe}^{2+}$ . That was the

reason for the high-efficiency of ferrous iron for As stabilization in AAR. In conclusion, the influence of coexisting soluble carbonate in AAR on As stabilization was insignificant in the ferrous iron system but significantly negative in the lime system.

### 3.5. Long-term stability of the treated AAR

The long-term stabilities of treated AAR samples were further investigated by comparing As leaching concentrations after 7 days and 1 year of curing. For the ferrous iron-treated AAR, As leaching concentration remained almost unchanged after a long time of curing (1.5 vs. 1.6 mg/L) (Fig. 6), showing a high long-term stability. In fact, during the long-term curing, Fe(II) in the ferrous iron-treated AAR was gradually oxidized by oxygen according to the results of XPS (Fig. S6). However, it was hard to distinguish the oxidation of Fe(II) in symplectite and siderite in this work. If symplectite was oxidized,  $\text{Fe}^{\text{II}}\text{Fe}^{\text{III}}(\text{AsO}_4)_2(\text{OH})_2 \cdot 6\text{H}_2\text{O}$  or ferrisymplesite ( $\text{Fe}_3^{\text{III}}(\text{AsO}_4)_2(\text{OH})_3 \cdot 5\text{H}_2\text{O}$ ) may be formed by analogy with the oxidation of vivianite ( $\text{Fe}_3(\text{PO}_4)_2 \cdot 8\text{H}_2\text{O}$ ) in air (Raghav et al., 2013; Rothe et al., 2016). Symplectite and oxidized symplectite were reported to display similar As leaching behavior (Raghav et al., 2013). Demopoulos's group found that oxidation of Fe(II)-As(V) precipitates could cause a slight release of As, but the released As would be re-stabilized via re-adsorption or formation of ferric arsenate (Doerfelt et al., 2015). Meanwhile, Jönsson and Sherman stated that symplectite was much more resistant to oxidation than siderite, implying that siderite was able to protect symplectite against oxidation (Jönsson and Sherman, 2008). The presence of siderite could enhance the long-term stability of symplectite in the ferrous iron-treated AAR when exposed to air. Overall, the mechanisms for the great long-term stability of ferrous iron-treated AAR were complicated and required further studies.

In contrast, the long-term stability of lime-treated AAR was unsatisfactory after 1 year of curing, with an increase of As leaching concentration to 15 mg/L (Fig. 6). This is due to the slow decomposition of calcium arsenate minerals to form calcium carbonate and soluble arsenate when exposed to atmospheric  $\text{CO}_2$  (Drahota and Filipi, 2009; Nazari et al., 2017). The XRD results (Fig. S7) confirmed that the decomposition of calcium arsenate with elevated calcium carbonate after 1 year of curing. Therefore, the long-term stability of ferrous iron-treated AAR is far superior to that of lime-treated AAR when exposed to air.

## 4. Conclusion

Ferrous salts and lime as stabilizing agents of As have been investigated for AAR with a high content of coexisting carbonate in this study. The results demonstrate that ferrous iron is more efficient than lime for AAR stabilization to reduce As leaching concentration lower than the limit value of 2.5 mg/L. The required dosage of ferrous iron was only one-tenth of that of lime. The stabilization mechanism was predominantly associated with the formation of arsenate minerals, ferrous arsenate or calcium arsenate. The difference in efficiency was mainly attributed to the different reaction pathways in ferrous iron and lime systems. Because of the coexisting soluble carbonate, the formation of ferrous arsenate was prior to that of ferrous carbonate in the ferrous iron system, whereas calcium arsenate was formed only after the saturation of calcium carbonate in the lime system. Thus, the presence of coexisting soluble carbonate decided that ferrous salts were preferred than lime as the stabilizing agents for AAR. These findings indicate that it's critical to select suitable stabilizing agents based on the nature of wastes. This study provides a facile and green stabilization scheme for AAR, as well as other similar As-bearing solid wastes with high contents of arsenate and carbonate, such as solid wastes from the basic refining process of blister copper and other metals (Hao et al., 2017; Kucharski, 2002).

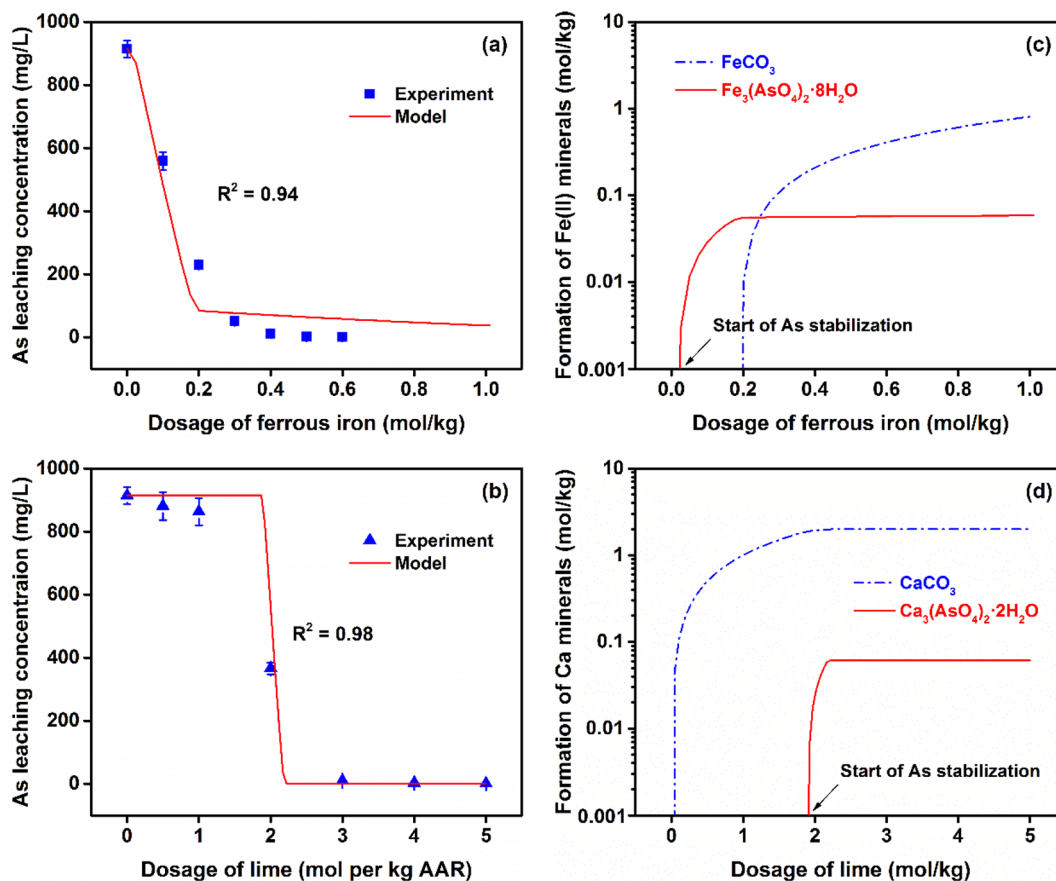


Fig. 5. Thermodynamic modeling results of As stabilization in AAR by ferrous iron (as  $\text{FeSO}_4$ ) and lime after 7 days of curing. (a, b) Variation of As leaching concentration as a function of dosages of stabilizing agents; (c, d) Formation sequences of arsenate and carbonate minerals as a function of dosages of stabilizing agents.

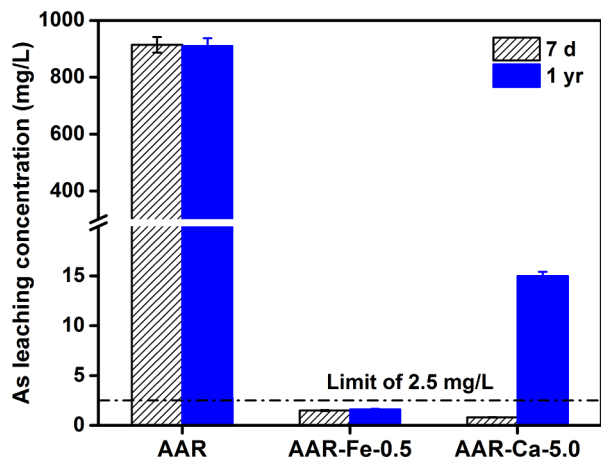


Fig. 6. Long-term stability of the treated AAR. The dosages of ferrous iron (as  $\text{FeSO}_4$ ) and lime were 0.5 and 5.0 mol/kg AAR, respectively.

#### CRediT authorship contribution statement

**Xin Wang:** Conceptualization, Methodology, Writing - original draft. **Jiaqi Ding:** Investigation, Validation. **Linling Wang:** Conceptualization, Writing - review & editing. **Shuyuan Zhang:** Investigation. **Huijie Hou:** Writing - review & editing. **Jingdong Zhang:** Supervision. **Jing Chen:** Funding acquisition, Resources. **Miao Ma:** Investigation. **Daniel C.W. Tsang:** Writing - review & editing. **Xiaohui Wu:** Supervision.

#### Declaration of Competing Interest

The authors of this publication are Xin Wang, Jiaqi Ding, Linling Wang, Shuyuan Zhang, Huijie Hou, Jingdong Zhang, Jing Chen, Miao Ma, Daniel C.W. Tsang, and Xiaohui Wu. All authors are aware and have consented to this submission. No conflict of interest exists in the submission of this manuscript.

#### Acknowledgments

This work was supported by the National Natural Science Foundation of China (No. 41671311), the China Scholarship Council (Grant No. 201806165010), and the Program for HUST Academic Frontier Youth Team (No. 2018QYTD05). The authors would like to thank the Analytical and Testing Center at Huazhong University of Science and Technology, and the Geological Experimental Testing Center of Hubei Province, China, for their assistance on sample characterization. We also acknowledge the kind help of Dr. Aimal Khan.

#### Appendix A. Supplementary material

Supplementary data to this article can be found online at <https://doi.org/10.1016/j.envint.2019.105406>.

#### References

- Anderson, C.G., 2012. The metallurgy of antimony. *Chem. Erde* 72, 3–8. <https://doi.org/10.1016/j.chemer.2012.04.001>.
- Arai, Y., Sparks, D.L., Davis, J.A., 2004. Effects of dissolved carbonate on arsenate adsorption and surface speciation at the hematite–water interface. *Environ. Sci. Technol.* 38, 817–824. <https://doi.org/10.1021/es034800w>.

- Beiyuan, J., Awad, Y.M., Beckers, F., Tsang, D.C.W., Ok, Y.S., Rinklebe, J., 2017. Mobility and phytoavailability of As and Pb in a contaminated soil using pine sawdust biochar under systematic change of redox conditions. *Chemosphere* 178, 110–118. <https://doi.org/10.1016/j.chemosphere.2017.03.022>.
- Bothe, J.V., Brown, P.W., 1999a. Arsenic immobilization by calcium arsenate formation. *Environ. Sci. Technol.* 33, 3806–3811. <https://doi.org/10.1021/es980998m>.
- Bothe, J.V., Brown, P.W., 1999b. The stabilities of calcium arsenates at  $23 \pm 1$  °C. *J. Hazard. Mater.* 69, 197–207. [https://doi.org/10.1016/S0304-3894\(99\)00105-3](https://doi.org/10.1016/S0304-3894(99)00105-3).
- Cao, M., Ye, Y., Chen, J., Lu, X., 2016. Remediation of arsenic contaminated soil by coupling oxalate washing with subsequent ZVI/Air treatment. *Chemosphere* 144, 1313–1318. <https://doi.org/10.1016/j.chemosphere.2015.09.105>.
- Catalano, J.G., Luo, Y., Otemuyiwa, B., 2011. Effect of aqueous Fe(II) on arsenate sorption on goethite and hematite. *Environ. Sci. Technol.* 45, 8826–8833. <https://doi.org/10.1021/es202445w>.
- Chen, D., Hu, H., Xu, Z., Liu, H., Cao, J., Shen, J., Yao, H., 2015. Findings of proper temperatures for arsenic capture by CaO in the simulated flue gas with and without SO<sub>2</sub>. *Chem. Eng. J.* 267, 201–206. <https://doi.org/10.1016/j.cej.2015.01.035>.
- Crittenden, J.C., Trussell, R.R., Hand, D.W., Howe, K.J., Tchobanoglous, G., 2012. *MWH's Water Treatment: Principles and Design*. John Wiley & Sons Inc, Hoboken, NJ, USA.
- Daenzer, R., Feldmann, T., Demopoulos, G.P., 2015. Oxidation of ferrous sulfate hydrolyzed slurry—kinetic aspects and impact on As(V) removal. *Ind. Eng. Chem. Res.* 54, 1738–1747. <https://doi.org/10.1021/ie503976k>.
- Daenzer, R., Xu, L., Doerfelt, C., Jia, Y., Demopoulos, G.P., 2014. Precipitation behaviour of As(V) during neutralization of acidic Fe(II)–As(V) solutions in batch and continuous modes. *Hydrometallurgy* 146, 40–47. <https://doi.org/10.1016/j.hydromet.2014.03.005>.
- Deng, W.H., Chai, L.Y., Dai, Y.J., 2014. Industrial experimental study on comprehensive recovering valuable resources from antimony smelting arsenic alkali residue. *Hunan Nonferrous Metals* 30, 24–27.
- Doerfelt, C., Feldmann, T., Daenzer, R., Demopoulos, G.P., 2015. Stability of continuously produced Fe(II)/Fe(III)/As(V) co-precipitates under periodic exposure to reducing agents. *Chemosphere* 138, 239–246. <https://doi.org/10.1016/j.chemosphere.2015.05.096>.
- Drahotka, P., Filippi, M., 2009. Secondary arsenic minerals in the environment: a review. *Environ. Int.* 35, 1243–1255. <https://doi.org/10.1016/j.envint.2009.07.004>.
- Guo, X., Wang, K., He, M., Liu, Z., Yang, H., Li, S., 2014. Antimony smelting process generating solid wastes and dust: characterization and leaching behaviors. *J. Environ. Sci.* 26, 1549–1556. <https://doi.org/10.1016/j.jes.2014.05.022>.
- Hao, Z.F., Shen, Q.H., Chen, W., 2017. The method of removing arsenic and antimony from blister copper. *Mining Metall.* 26, 59–62.
- Haynes, W.M., 2014. *CRC Handbook of Chemistry and Physics*. CRC Press, Boca Raton, Fla, USA.
- Huo, L., Zeng, X., Su, S., Bai, L., Wang, Y., 2017. Enhanced removal of As(V) from aqueous solution using modified hydrous ferric oxide nanoparticles. *Sci. Rep.* 7, 40765. <https://doi.org/10.1038/srep40765>.
- Jönsson, J., Sherman, D.M., 2008. Sorption of As(III) and As(V) to siderite, green rust (ferugite) and magnetite: implications for arsenic release in anoxic groundwaters. *Chem. Geol.* 255, 173–181. <https://doi.org/10.1016/j.chemgeo.2008.06.036>.
- Johnston, R.B., Singer, P.C., 2007. Solubility of symplectite (ferrous arsenate): implications for reduced groundwaters and other geochemical environments. *Soil Sci. Soc. Am. J.* 71, 101–107. <https://doi.org/10.2136/sssaj2006.0023>.
- Jones, R.G., Loepfert, R.H., 2013. Calcite surface adsorption of As(V), As(III), MMAs(V), and DMAs(V) and the impact of calcium and phosphate. *Soil Sci. Soc. Am. J.* 77, 83–93. <https://doi.org/10.2136/sssaj2012.0052>.
- Kanematsu, M., Young, T.M., Fukushi, K., Sverjensky, D.A., Green, P.G., Darby, J.L., 2011. Quantification of the effects of organic and carbonate buffers on arsenate and phosphate adsorption on a goethite-based granular porous adsorbent. *Environ. Sci. Technol.* 45, 561–568. <https://doi.org/10.1021/es1026745>.
- Kucharski, M., 2002. Arsenic removal from blister copper by soda injection into melts. *Scand. J. Metall.* 31, 246–250. <https://doi.org/10.1034/j.1600-0692.2002.00534.x>.
- Kumpiene, J., Lagerkvist, A., Maurice, C., 2008. Stabilization of As, Cr, Cu, Pb and Zn in soil using amendments – a review. *Waste Manage.* 28, 215–225. <https://doi.org/10.1016/j.wasman.2006.12.012>.
- Kundu, S., Gupta, A.K., 2008. Immobilization and leaching characteristics of arsenic from cement and/or lime solidified/stabilized spent adsorbent containing arsenic. *J. Hazard. Mater.* 153, 434–443. <https://doi.org/10.1016/j.jhazmat.2007.08.073>.
- Lei, J., Peng, B., Liang, Y.-J., Min, X.-B., Chai, L.-Y., Ke, Y., You, Y., 2018. Effects of anions on calcium arsenate crystalline structure and arsenic stability. *Hydrometallurgy* 177, 123–131. <https://doi.org/10.1016/j.hydromet.2018.03.007>.
- Li, J.-S., Wang, L., Cui, J.-L., Poon, C.S., Beiyuan, J., Tsang, D.C.W., Li, X.-D., 2018. Effects of low-alkalinity binders on stabilization/solidification of geogenic As-containing soils: spectroscopic investigation and leaching tests. *Sci. Total Environ.* 631–632, 1486–1494. <https://doi.org/10.1016/j.scitotenv.2018.02.247>.
- Li, Y., Wang, J., Peng, X., Ni, F., Luan, Z., 2012. Evaluation of arsenic immobilization in red mud by CO<sub>2</sub> or waste acid acidification combined ferrous (Fe<sup>2+</sup>) treatment. *J. Hazard. Mater.* 199–200, 43–50. <https://doi.org/10.1016/j.jhazmat.2011.10.055>.
- Li, Z., Chen, W.M., Jin, C.Y., 2015. The process research for separation of arsenic-alkali residue by fractional crystallization. *Hunan Nonferrous Metals* 31, 23–28.
- Liang, Y., Min, X., Chai, L., Wang, M., Liyang, W., Pan, Q., Okido, M., 2017. Stabilization of arsenic sludge with mechanochemically modified zero valent iron. *Chemosphere* 168, 1142–1151. <https://doi.org/10.1016/j.chemosphere.2016.10.087>.
- Miretzky, P., Cirelli, A.F., 2010. Remediation of arsenic-contaminated soils by iron amendments: a review. *Crit. Rev. Env. Sci. Technol.* 40, 93–115. <https://doi.org/10.1080/10643380802202059>.
- Moon, D., Dermatas, D., Menounou, N., 2004. Arsenic immobilization by calcium–arsenic precipitates in lime treated soils. *Sci. Total Environ.* 330, 171–185. <https://doi.org/10.1016/j.scitotenv.2004.03.016>.
- Multani, R.S., Feldmann, T., Demopoulos, G.P., 2016. Antimony in the metallurgical industry: a review of its chemistry and environmental stabilization options. *Hydrometallurgy* 164, 141–153. <https://doi.org/10.1016/j.hydromet.2016.06.014>.
- Nazari, A.M., Radzinski, R., Ghahreman, A., 2017. Review of arsenic metallurgy: treatment of arsenical minerals and the immobilization of arsenic. *Hydrometallurgy* 174, 258–281. <https://doi.org/10.1016/j.hydromet.2016.10.011>.
- Pan, H., Hou, H., Shi, Y., Li, H., Chen, J., Wang, L., Crittenden, J.C., 2018. High catalytic oxidation of As(III) by molecular oxygen over Fe-loaded silicon carbide with MW activation. *Chemosphere* 198, 537–545. <https://doi.org/10.1016/j.chemosphere.2018.01.116>.
- Raghav, M., Shan, J., Sáez, A.E., Ela, W.P., 2013. Scoping candidate minerals for stabilization of arsenic-bearing solid residuals. *J. Hazard. Mater.* 263, 525–532. <https://doi.org/10.1016/j.jhazmat.2013.10.009>.
- Randall, P.M., 2012. Arsenic encapsulation using Portland cement with ferrous sulfate/lime and Terra-Bond™ technologies — microcharacterization and leaching studies. *Sci. Total Environ.* 420, 300–312. <https://doi.org/10.1016/j.scitotenv.2011.12.066>.
- Renew, J.E., Huang, C.-H., Burns, S.E., Carrasquillo, M., Sun, W., Ellison, K.M., 2016. Immobilization of heavy metals by solidification/stabilization of co-disposed flue gas desulfurization brine and coal fly ash. *Energy Fuels* 30, 5042–5051. <https://doi.org/10.1021/acs.energyfuels.6b00321>.
- Rothe, M., Kleeberg, A., Hupfer, M., 2016. The occurrence, identification and environmental relevance of vivianite in waterlogged soils and aquatic sediments. *Earth Sci. Rev.* 158, 51–64. <https://doi.org/10.1016/j.earscirev.2016.04.008>.
- Sø, H.U., Postma, D., Jakobsen, R., Larsen, F., 2008. Sorption and desorption of arsenate and arsenite on calcite. *Geochim. Cosmochim. Acta* 72, 5871–5884. <https://doi.org/10.1016/j.gca.2008.09.023>.
- Schecher, W.D., McAvoy D.C., 2007. *A Chemical Equilibrium Modeling System, Version 4.6*, Environmental Research Software, Hallowell, ME, USA.
- Stachowicz, M., Hiemstra, T., van Riemsdijk, W.H., 2007. Arsenic – bicarbonate interaction on goethite particles. *Environ. Sci. Technol.* 41, 5620–5625. <https://doi.org/10.1021/es063087i>.
- Tong, M., Yuan, S., Zhang, P., Liao, P., Alshawabkeh, A.N., Xie, X., Wang, Y., 2014. Electrochemically induced oxidative precipitation of Fe(II) for As(III) oxidation and removal in synthetic groundwater. *Environ. Sci. Technol.* 48, 5145–5153. <https://doi.org/10.1021/es500409m>.
- Wang, J., Xiao, Y.L., Wang, H.H., 2013. Analysis of the characteristics of the waterborne arsenic poisoning caused by arsenic-alkali residue from antimony metallurgical enterprise in human and its control countermeasures. *Pract. Prevent. Med.* 20, 150–152.
- Wang, L., Chen, L., Cho, D.-W., Tsang, D.C.W., Yang, J., Hou, D., Baek, K., Kua, H.W., Poon, C.-S., 2019a. Novel synergy of Si-rich minerals and reactive MgO for stabilization/solidification of contaminated sediment. *J. Hazard. Mater.* 365, 695–706. <https://doi.org/10.1016/j.jhazmat.2018.11.067>.
- Wang, L., Chen, L., Tsang, D.C.W., Kua, H.W., Yang, J., Ok, Y.S., Ding, S., Hou, D., Poon, C.S., 2019b. The roles of biochar as green admixture for sediment-based construction products. *Cem. Concr. Compos.* 104, 103348. <https://doi.org/10.1016/j.cemconcomp.2019.103348>.
- Wang, L., Cho, D.-W., Tsang, D.C.W., Cao, X., Hou, D., Shen, Z., Alessi, D.S., Ok, Y.S., Poon, C.-S., 2019c. Green remediation of As and Pb contaminated soil using cement-free clay-based stabilization/solidification. *Environ. Int.* 126, 336–345. <https://doi.org/10.1016/j.envint.2019.02.057>.
- Wang, P., Liu, Y., Menzies, N.W., Wehr, J.B., de Jonge, M.D., Howard, D.L., Kopittke, P.M., Huang, L., 2016. Ferric minerals and organic matter change arsenic speciation in copper mine tailings. *Environ. Pollut.* 218, 835–843. <https://doi.org/10.1016/j.envpol.2016.08.007>.
- Wang, X., Zhang, J., Wang, L., Chen, J., Hou, H., Yang, J., Lu, X., 2017. Long-term stability of FeSO<sub>4</sub> and H<sub>2</sub>SO<sub>4</sub> treated chromite ore processing residue (COPR): importance of H<sup>+</sup> and SO<sub>4</sub><sup>2-</sup>. *J. Hazard. Mater.* 321, 720–727. <https://doi.org/10.1016/j.jhazmat.2016.09.048>.
- Wang, X., Zhang, H., Wang, L., Chen, J., Xu, S., Hou, H., Shi, Y., Zhang, J., Ma, M., Tsang, D.C.W., Crittenden, J.C., 2019. Transformation of arsenic during realgar tailings stabilization using ferrous sulfate in a pilot-scale treatment. *Sci. Total Environ.* 668, 32–39. <https://doi.org/10.1016/j.scitotenv.2019.02.289>.
- Wen, B., Zhou, A., Zhou, J., Liu, C., Huang, Y., Li, L., 2018. Coupled S and Sr isotope evidences for elevated arsenic concentrations in groundwater from the world's largest antimony mine, Central China. *J. Hydrol.* 557, 211–221. <https://doi.org/10.1016/j.jhydrol.2017.12.013>.
- Yang, L., Donahoe, R.J., Redwine, J.C., 2007. In situ chemical fixation of arsenic-contaminated soils: an experimental study. *Sci. Total Environ.* 387, 28–41. <https://doi.org/10.1016/j.scitotenv.2007.06.024>.
- Zeng, G.S., Li, H., Chen, S.H., Tu, X.M., Wang, W.B., 2011. Leaching kinetics and separation of antimony and arsenic from arsenic alkali residue. *Adv. Mater. Res.* 402, 57–60. <https://doi.org/10.4028/www.scientific.net/amr.402.57>.
- Zhong, D., Jiang, Y., Zhao, Z., Wang, L., Chen, J., Ren, S., Liu, Z., Zhang, Y., Tsang, D.C.W., Crittenden, J.C., 2019. pH dependence of arsenic oxidation by rice-husk-derived biochar: roles of redox-active moieties. *Environ. Sci. Technol.* 53, 9034–9044. <https://doi.org/10.1021/acs.est.9b00756>.
- Zhu, Y.N., Zhang, X.H., Xie, Q.L., Wang, D.Q., Cheng, G.W., 2006. Solubility and stability of calcium arsenates at 25 °C. *Water Air Soil Pollut.* 169, 221–238. <https://doi.org/10.1007/s11270-006-2099-y>.